Journal Name

COMMUNICATION

Supporting Information

KNH_2 - KH: a metal amide - hydride solid solution

Antonio Santoru*, Claudio Pistidda, Magnus H. Sørby, Michele R. Chierotti, Sebastiano Garroni, Eugenio Pinatel, Fahim Karimi, Hujun Cao, Paolo C. Vioglio, Nils Bergemann, Thi T. Le, Julián Puszkiel, Roberto Gobetto, Marcello Baricco, Bjørn C. Hauback, Thomas Klassen and Martin Dornheim

Experimental details.

Synthesis. KH (30 wt% dispersion in mineral oil) was purchased from Sigma-Aldrich. Before usage the oil was removed by washing 3 times with hexane in vacuum filtration. KNH_2 was synthesized by reactive ball milling of the dry potassium hydride powder in a Fritsch Pulverisette 6, at 400 RPM, with a BPR ca. 20:1, under 7 bar of ammonia atmosphere. The reaction vessel (a high pressure vial from Evicomagnetics) was evacuated and refilled with ammonia 4 times, for a total milling time of 18 h. Both the starting materials (KH and KNH_2) were then independently ball milled in a SPEX 8000 mill for 600 minutes to obtain a finer powder. The mixtures of KNH_2 and KH were prepared grinding the two reactants for 5 minutes in an agate mortar. The annealed samples were prepared in a thermal reactor from Parr Instruments, heating at 270 °C under Argon atmosphere for 1 h.
The ball milled samples were prepared using a SPEX 8000 Mill, milling the powder for 5h with a BPR of 10:1. Hardened steel vials and balls were used.
Potassium deuteramide (KND_2) was synthesized by thermal treatment of metallic potassium under 5 bar of deuterated ammonia (ND_3) for 16 h at 300 °C in an autoclave from Parr Instruments. The reaction can be written as: $K + ND_3 \rightarrow KND_2 + 1 / 2\ D_2$
Potassium deuteride was synthesize ball milling pure potassium under 50 bar of deuterium (D_2) for 36 h with a rotational speed of 600 rpm and a ball to powder ratio of 60:1. Potassium (98 % purity) under mineral oil was purchased as commercial product from Sigma Aldrich. A cube of 1.1 g approximately was cut. Before use, the oil was removed washing with hexane. In addition the material surface was polished with a sharp blade.
The diffractograms on the ball milled samples (Figure S2) were collected with a Bruker D8 Advance diffractometer in Bragg-Brentano geometry using a General Area detector and a Cu X-ray source. The sample was investigated using an airtight sample holder from Bruker. The incoherent scattering of the Poly (methyl methacrylate) dome is responsible for the bump observed between 1 and 2 $Å^{-1}$ in all the diffractograms (Figure S2).
The diffractograms on the annealed samples (Figure S3) were performed in the 2θ range 2° – 90° (step size of 0.017°, time per step 200 s) using a laboratory diffractometer (Panalytical X'Pert Pro Multipurpose Diffractometer) equipped with Ni filtered Cu source in Debye-Scherrer geometry. Samples were sealed into boron silica glass capillaries of internal diameter 0.8 mm in a protected atmosphere.
The sample handling was performed in an Argon circulation glove box, with oxygen and moisture concentrations lower than 2 ppm.
The scattering images obtained by *in situ* synchrotron X-ray diffraction were integrated with the program Fit2D.[1] Rietveld refinement was performed by means of MAUD program (Material Analysis Using Diffraction)[2] on the diffractograms selected for phase identification and determination of the cell parameters (Figures S5, S6, S7, S8, S9). In any case structural models from the literature were used for the known phases of KNH_2 and KH. For the new $K(NH_2)_xH_{(1-x)}$ phases a general structural model was obtained using FOX software[3] on the pattern obtained by *in situ* powder neutron diffraction on the sample with nominal composition x = 0.5 and then adapted for the other different compositions. The occupancies for the amide and hydride anions were calculated and fixed in order to be in agreement with the refined composition of the room temperature pattern. The Rietveld refinement of the neutron diffraction pattern was performed with GSAS software.[4]

Linear expansion coefficients and related structural properties.

The linear thermal expansion coefficients reported in Table 1 were calculated according to the following formula:
$\alpha_L = (a_2 - a_1) / [a_1 (T_2 - T_1)]$, where $T_2 > T_1$ and $a_2 > a_1$.

The cell parameters "a_1" and the temperatures "T_1" are referred to the diffractograms collected during the cooling process, since in that interval only one $K(NH_2)_xH_{(1-x)}$ was present. T_2 = 270 °C for all the samples. For the compositions x = 0, 0.1, 0.3, 0.5, 0.7 the calculations are referred to $T_1 \approx$ RT while for the compositions x = 0.9 and x = 1, the diffractograms corresponding to T_1 = 48 °C and T_1 = 82 °C were selected respectively, due to the phase transformations occurring at lower temperatures.
The obtained linear expansion coefficient was then used to calculate the cell parameter expected at T_1 = 20 °C for the cubic polymorph of each composition (also reported in Table 1). Even though for the pure KNH_2 the cubic polymorph does not exist at room temperature (in normal pressure conditions), the cell parameter calculated with the linear expansion coefficient of the cubic form of KNH_2 is in good agreement with the values expected by the linear behavior (Figure 4 – Main article). The explanation most probably resides in the structural similarities between the different polymorphs of KNH_2. Indeed, considering the cubic structure highlighted in Figure S1, an element of pseudo-cubic symmetry with comparable interatomic distances can be easily identified also in the monoclinic and tetragonal polymorphs.

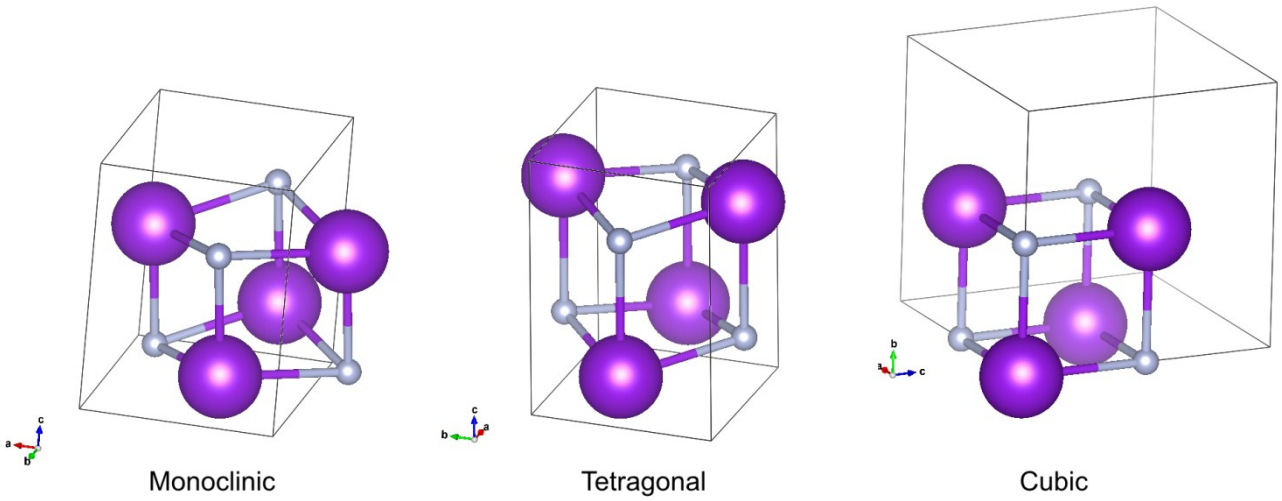

Figure S1. Structural similarities between the different polymorphs of KNH_2. The hydrogen atoms of the NH_2 groups were omitted for clarity.

Effect of ball milling
The interaction between KNH_2 and KH under mechanochemical or thermal input was studied for different compositions. The mechanical energy transfer induces a chemical reaction of the compounds already after 5 h. *Ex situ* PXD on the ball milled samples (Figure S2) shows a complete disappearance of the monoclinic polymorph of potassium amide. For all the compositions two different cubic structures coexist, namely an "amide rich" and a "hydride rich" structure. Noteworthy, the formation of a monoclinic polymorph is not observed even after several months.

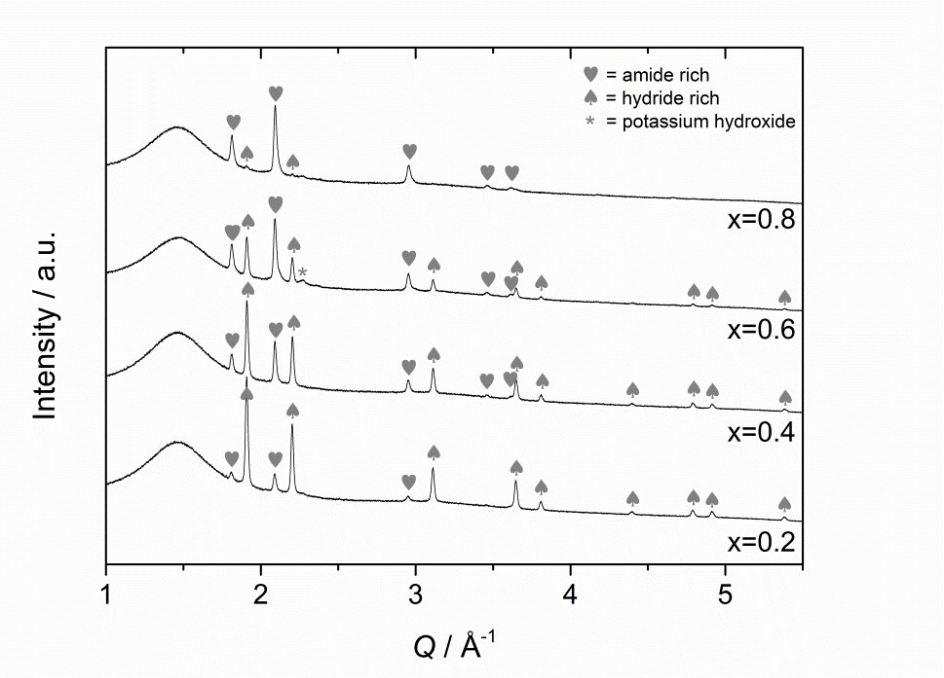

Figure S2. Diffractograms on the x KNH_2 + (1-x) KH samples collected after mechanochemical treatment.

Effect of annealing

The compositions 0.1, 0.3, 0.5, 0.7, 0.9 were studied promoting the reaction by thermal treatment up to 270 °C. *Ex situ* PXD on the annealed samples (Figure S3) confirmed that, also by thermal input, KNH_2 and KH mutually reacted to form at least two cubic phases (compositions x = 0.3, 0.5, 0.7) and only close to the lower extreme of the compositional range (x = 0.1) one single cubic phase was found, probably stabilized by the high relative amount of potassium hydride. For the composition x = 0.9, coexistence of the cubic and monoclinic phase was found. Due to the fact that amide anions can be hosted in a single cubic lattice only for certain compositions (approximately x = 0.1), these results suggest a two phase field at room temperature.

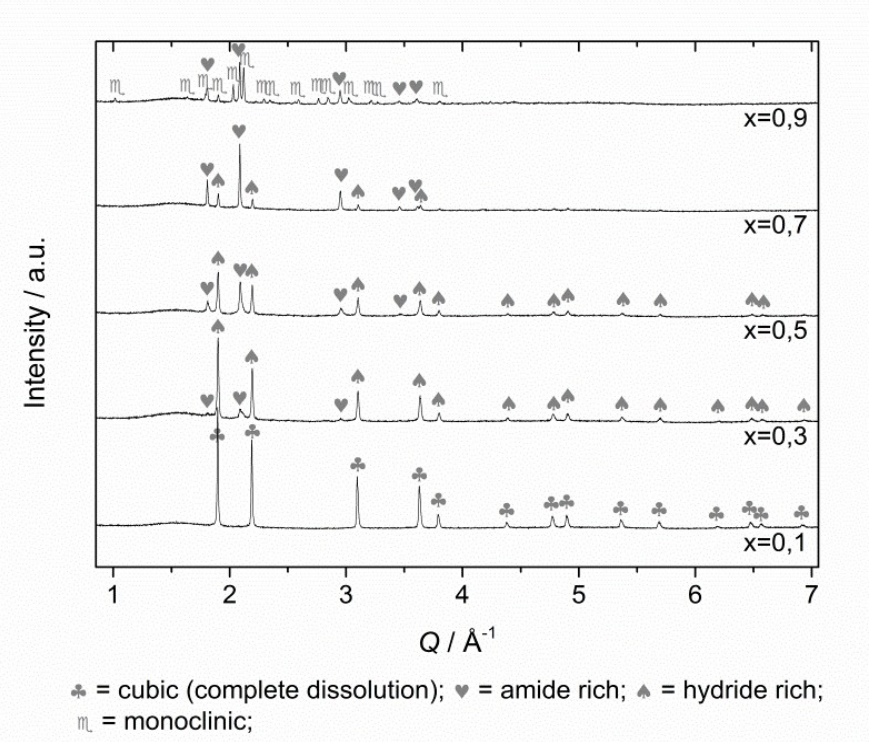

Figure S3. Room temperature diffractograms on the on the x KNH_2 + (1-x) KH samples collected after thermal treatment to 270 °C.

***In situ* synchrotron radiation powder X-ray diffraction (SR-PXD)**

In situ synchrotron X-ray diffraction experiments were performed on five selected compositions (x = 0.1, 0.3, 0.5, 0.7, 0.9), to investigate the behaviour of the K-N-H system upon heat treatment. The pure phases of KH and KNH_2 (indicated as x = 0 and x = 1 respectively) were also measured as reference (Figure S4).

For all the samples with intermediate compositions (x = 0.1, 0.3, 0.5, 0.7, 0.9) the phase transformations of KNH_2 takes place in the expected temperature region. At about 100 °C KNH_2 (F*m*-3*m*) and KH (F*m*-3*m*) are present. At higher temperatures, the change of the diffracted intensities together with the different shift of KNH_2 peaks reveals the starting point of the reaction between the two phases. This reaction continues until ca. 270°C, with a gradual convergence of the two starting structures (an amide-rich- and a hydride-rich phase) to the single phase composition.

In the isothermal part, at 270 °C, the reaction is completed and only one cubic phase is present and appears to be stable for the entire isothermal period, since there are no significant changes of the peaks positions and intensities, independently from the composition. The formation of a single phase for all the compositions is a confirmation of the stability of the solid solution at 270 °C. During the cooling process the only noticeable change is the expected contraction of the cell for the nominal compositions x = 0.1, 0.3, 0.5, 0.7. Only for the composition x = 0.9, a phase transformation to a tetragonal geometry occurs almost at room temperature. Interestingly, since only the tetragonal phase is present, a partial solubility of KH into the tetragonal polymorph of KNH_2 is demonstrated. The structural similarities (highlighted in Figure S1) between the cubic and tetragonal polymorphs are probably responsible for the solubility of small amounts of KH in the tetragonal KNH_2 phase. Moreover, a comparison of this result with the one obtained by *ex situ* PXD on the same composition measured several days after annealing (Figure S3 – x = 0.9) suggests a metastability of the tetragonal phase at room temperature. The solubility of KH in the tetragonal polymorph of KNH_2 could be explained considering the structural similarities between the different polymorphs (Figure S1). Concerning the compositions x = 0.3, 0.5, 0.7, during the cooling process in the *in situ* experiments the kinetic inertia of the system prevents the

single phase from disproportioning into two or more cubic phases, as it should be expected according to the *ex situ* data reported in Figure S3. The Rietveld refinements of the selected pattern at room temperature and at 270 °C are reported in the following figures (Figure S5, S6, S7, S8 and S9).

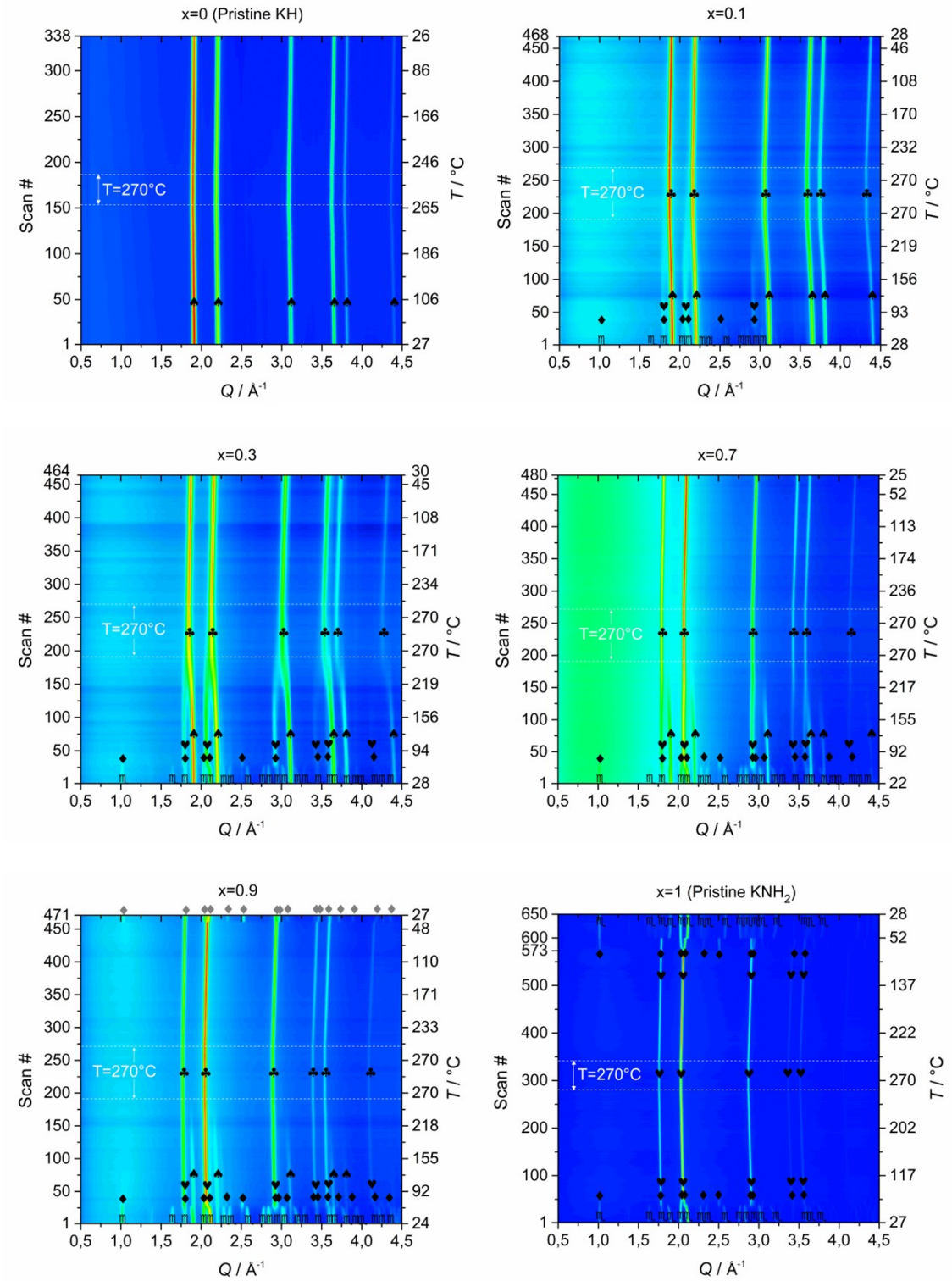

Figure S4. *In situ* SR-PXD measurements of all the compositions x KNH_2 + (1-x) KH (x = 0, 0.1, 0.3, 0.7, 0.9, 1) ℳ = KNH_2 (P121/m1), ♦ = KNH_2 (P4/nmm), ♥ = KNH_2 (Fm-3m), ♣ = $K(NH_2)_xH_{(1-x)}$ (Fm-3m), ♦ = $K(NH_2)_xH_{(1-x)}$ (P4/nmm).

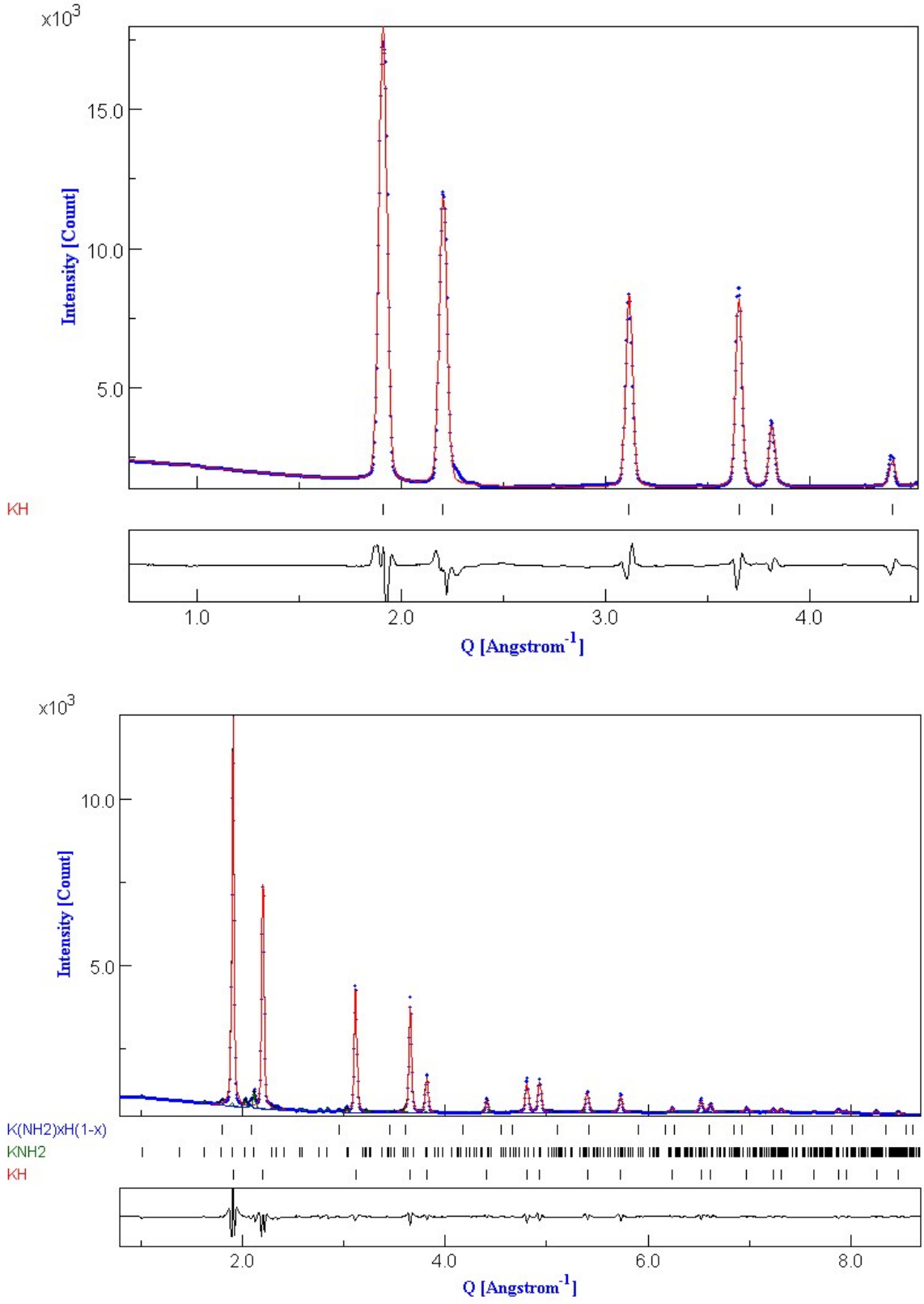

Figure S5. Rietveld refinement of the room temperature SR-PXD pattern of pristine KH (top) and the grinded x KNH_2 + (1 - x) KH sample of nominal composition x = 0.1 (bottom). Rw(%) = 5.01 and Rw(%) = 4.70 respectively.

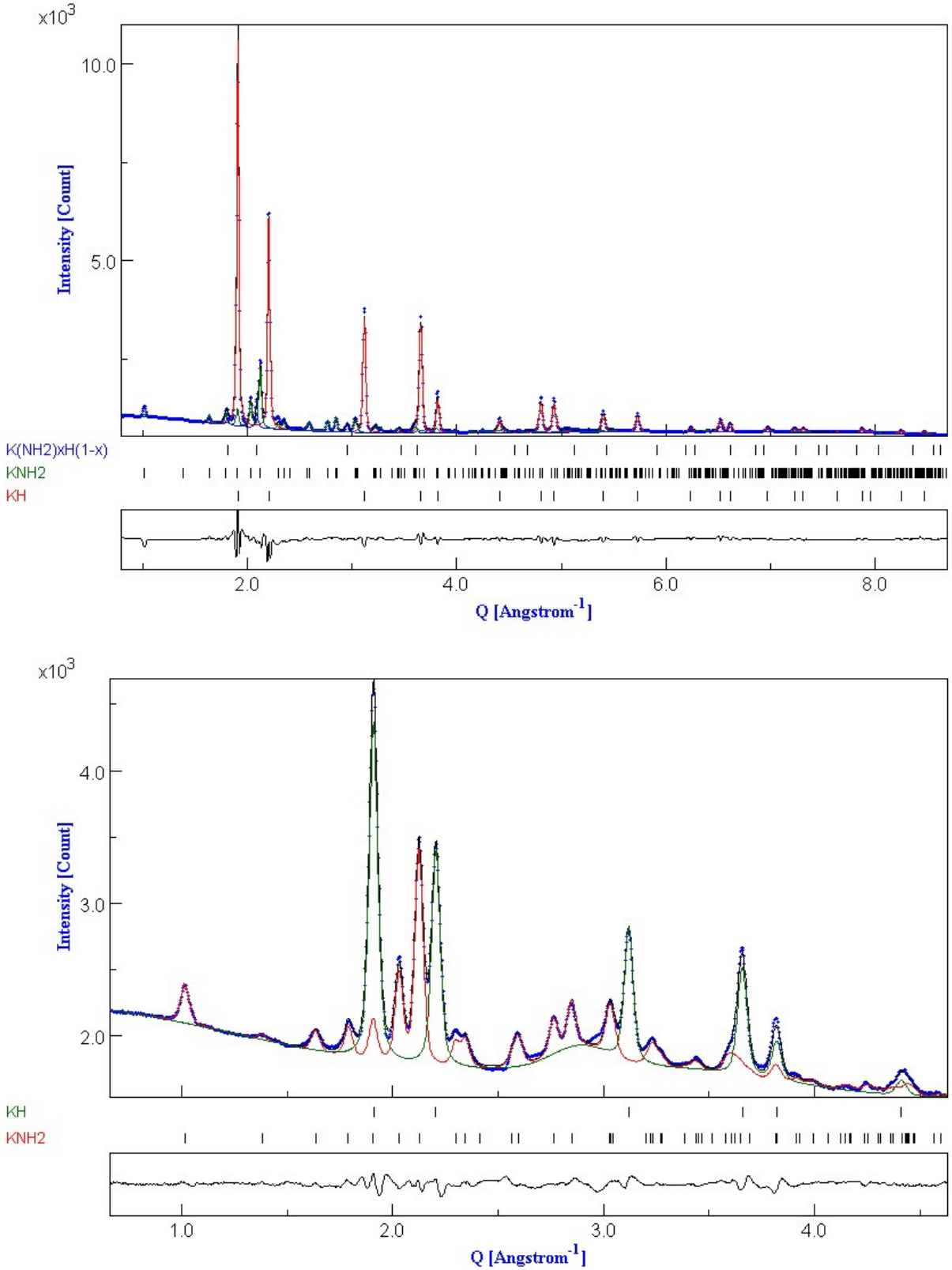

Figure S6. Rietveld refinement of the room temperature SR-PXD pattern of the grinded x KNH_2 + (1 - x) KH samples of nominal composition x = 0.3 (top) and x = 0.5 (bottom). Rw(%) = 4.95 and Rw(%) = 1.05 respectively.

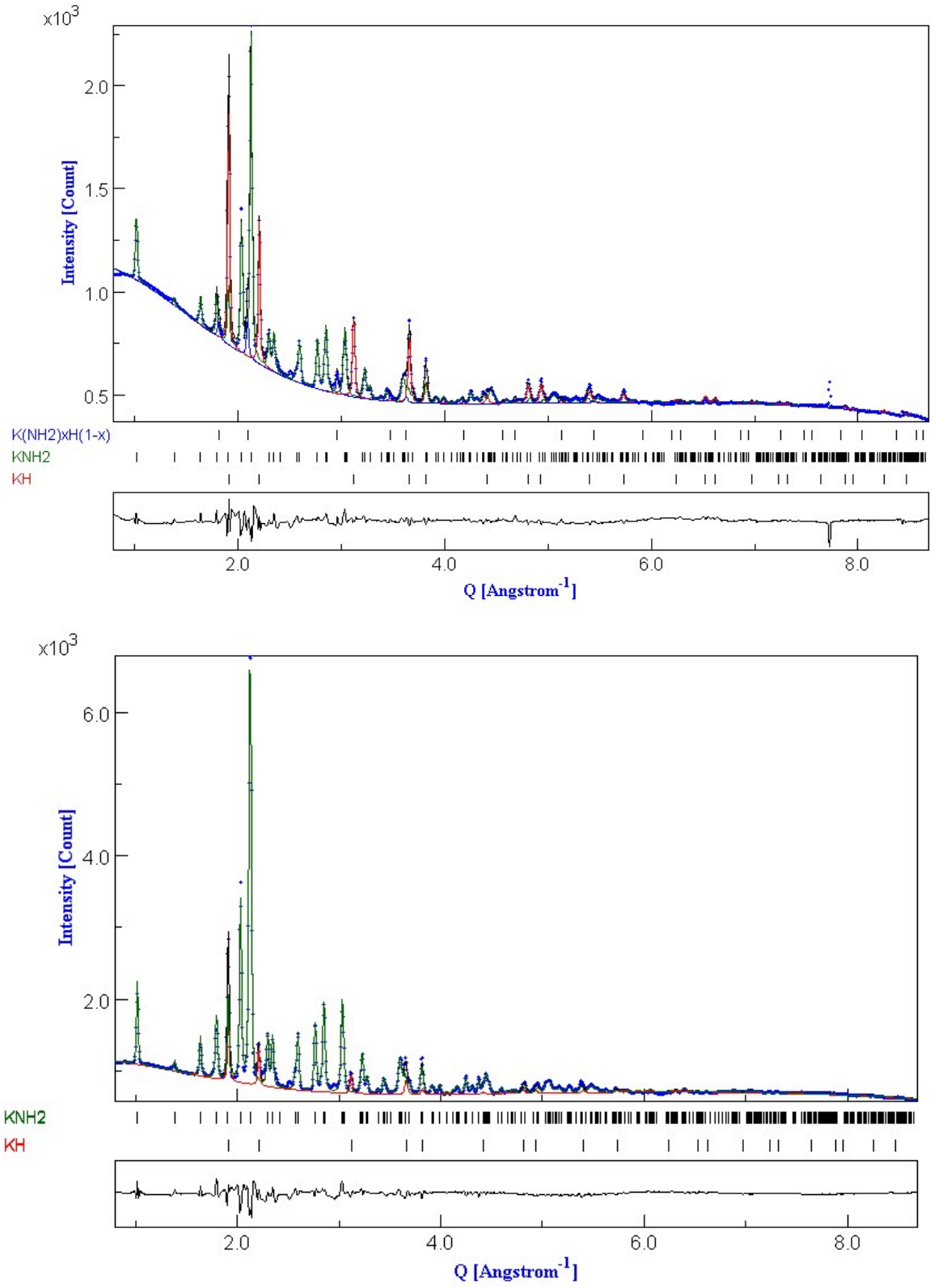

Figure S7. Rietveld refinement of the room temperature SR-PXD pattern of the grinded x KNH_2 + (1 - x) KH samples of nominal composition x = 0.7 (top) and x = 0.9 (bottom). Rw(%) = 2.14 and Rw(%) = 3.37 respectively.

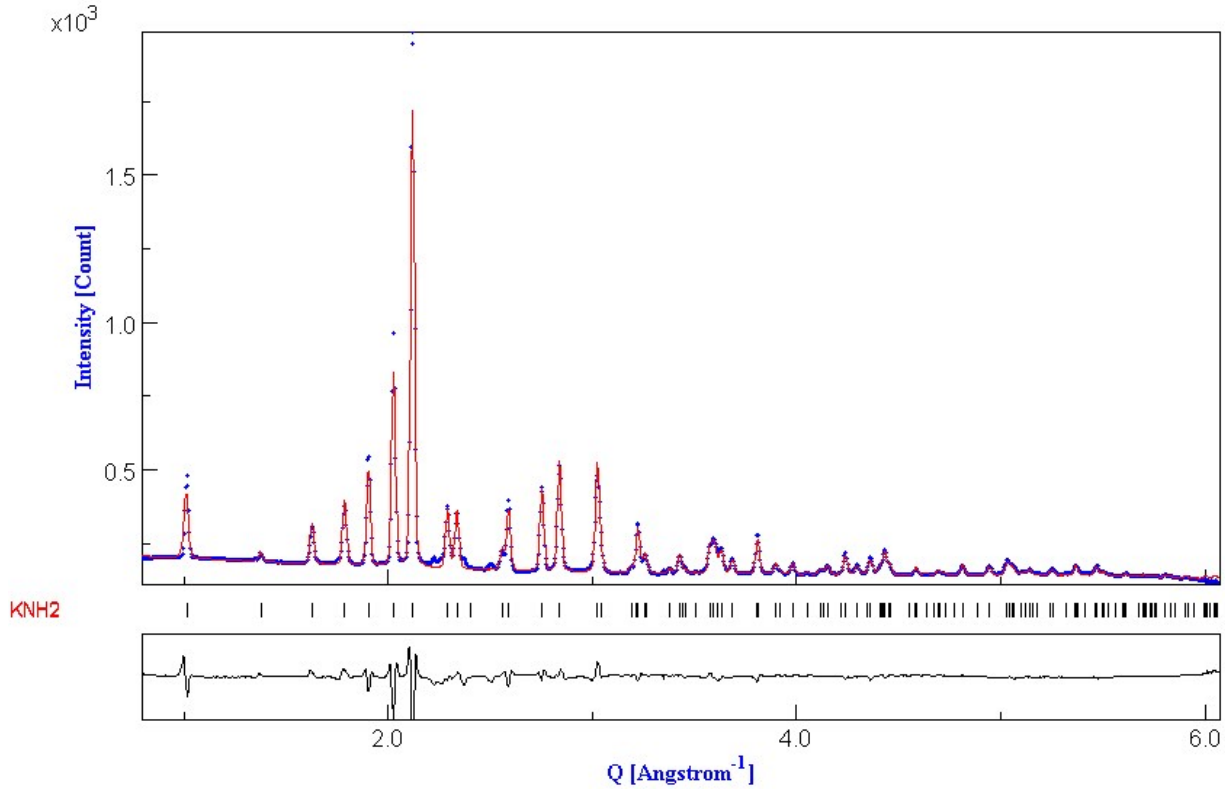

Figure S8. Rietveld refinement of the room temperature SR-PXD pattern of the as obtained KNH_2 sample. Rw(%) = 5.16.

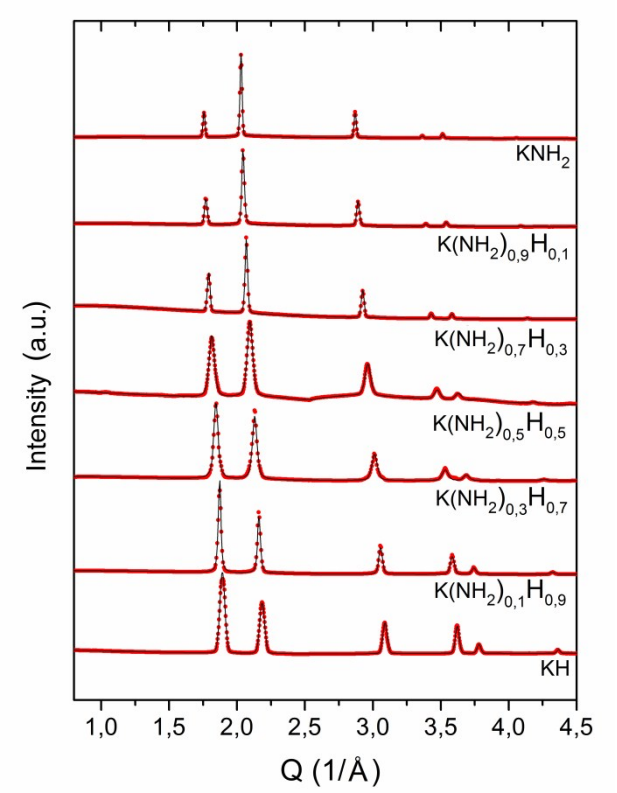

Figure S9. Rietveld refinements of the SR-PXD pattern collected at 270 °C for each composition,

High temperature powder neutron diffraction (PND)

The results obtained by *in situ* SR-PXD are confirmed also by PND on a deuterated sample of nominal composition x = 0.5. The sample was first measured at RT, then transferred in the high temperature cell and measured again in order to be able to remove the contribution of the sample holder by comparison (Figure S10). The sample was then heated up to 270 °C and kept in isotherm during the acquisition of the diffraction pattern.

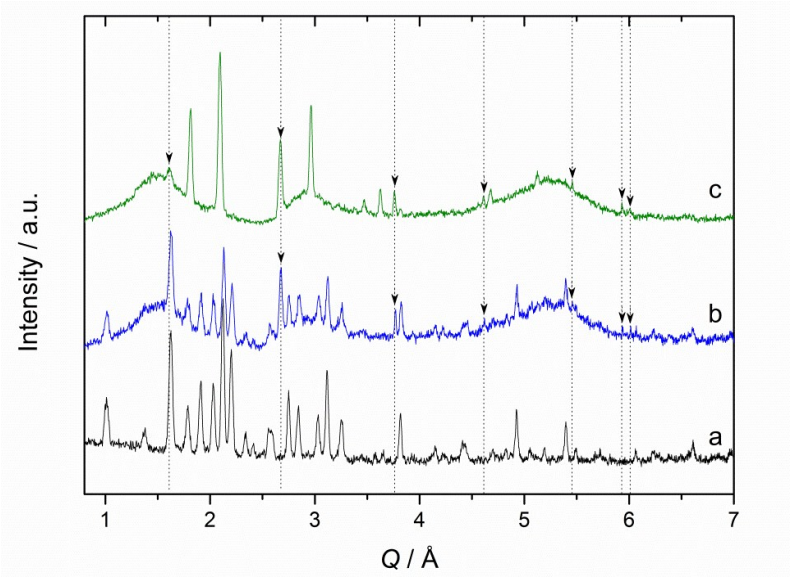

Figure S10. Powder neutron diffraction pattern of the samples 0.5 KND2 + 0.5 KD at RT inside of the vanadium sample holder (a), and the same sample at room temperature (b) and at 270 °C (c) when the quartz sample holder was employed. A wavy background and some new Bragg reflections can be noticed. The peaks generated from the quartz sample holder are indicated by the arrows on the dotted lines and their absence can be noticed in the pattern corresponding to the vanadium sample holder (a).

Figure S11 depicts the Rietveld refinement of the RT diffractogram obtained with the in situ cell.

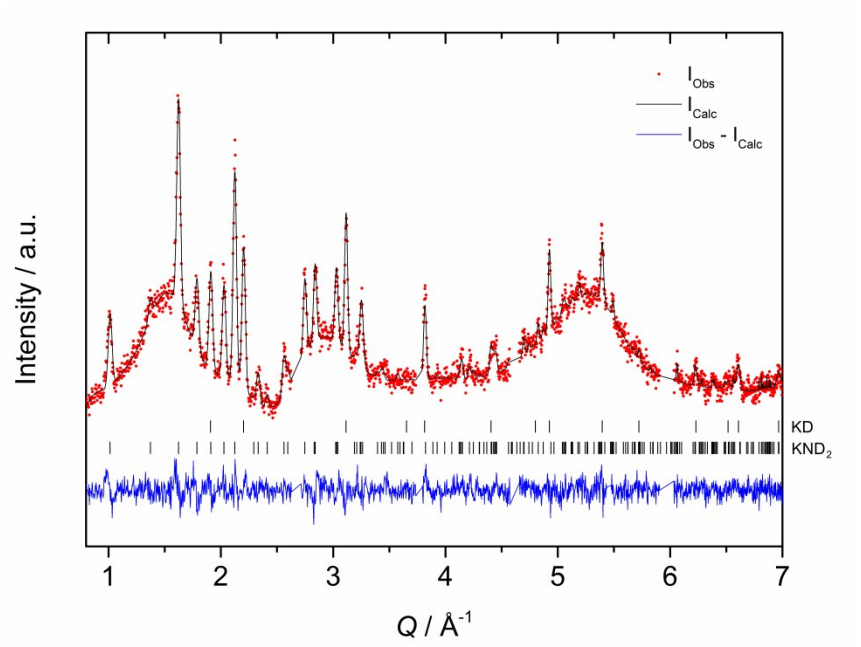

Figure S11. Rietveld refinement of the RT PND pattern of the sample 0.46 KND_2 + 0.54 KD. Rwp(%) = 5.52 (corrected for background).

Nuclear magnetic resonance

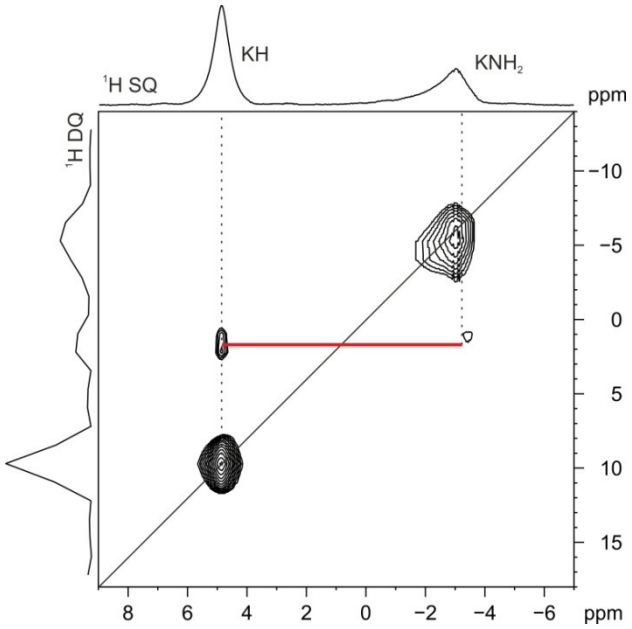

Figure S12. 2D ^{1}H (400.23 MHz) DQ MAS NMR spectrum of the KNH_2 + KH (x = 0.5) after grinding, recorded with a spinning speed of 32 kHz. The red line highlights the DQ correlation between the KH and KNH_2 signal.

Thermal decomposition

The thermal decomposition behavior of the solid solution was determined by differential thermal analysis (DTA) in a Netzsch STA 409 apparatus (Figure S13). After recording the baseline on an empty alumina crucible, about 8 mg of material were heated up in the same crucible under a flow of purified Argon of 50 mL_N/min.

The temperature was increased at 5 °C / min from RT up to 270 °C, kept constant for 10 minutes and then decreased to RT at the

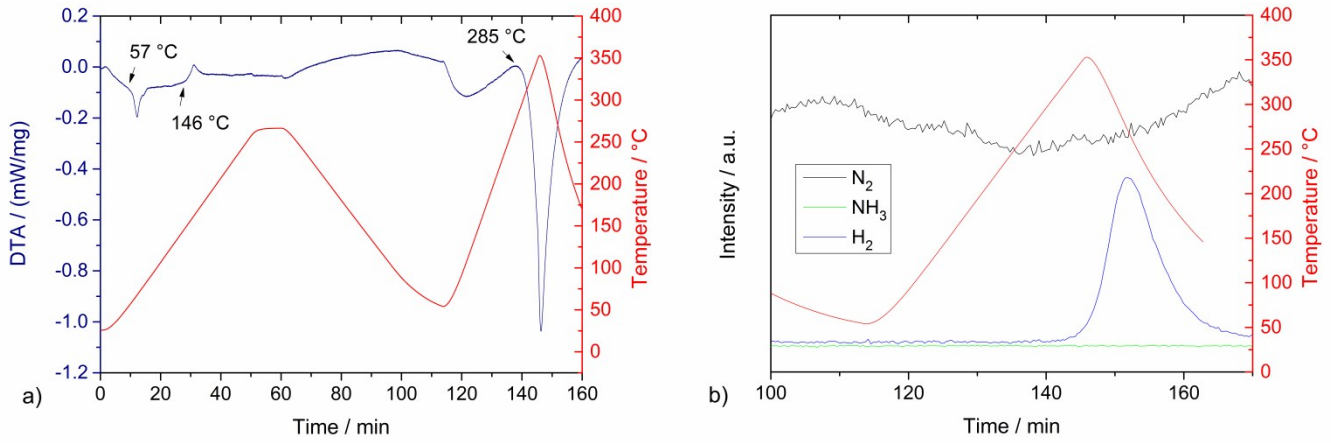

Figure S13. a) DTA measurement performed on the sample x = 0.5 and **b)** mass spectrometer signal during the decomposition process.

same rate in order to observe the formation of the solid solution. During this process an endothermic signal was recorded at ca. 57 °C which is close to the temperature value for the phase transition from the monoclinic to the tetragonal geometry. A less intense peak can be noticed in the shoulder of the main peak, accounting for the phase transition tetragonal → cubic. An exothermic event took place at 146 °C, most probably due to the formation of the solid solution. Right after the cooling process the temperature was increased up to 350 °C with a rate of 10 °C / min to observe the thermal decomposition. A strong endothermic signal can be noticed with an onset temperature of ca. 285 °C, which is ascribable to the starting of the thermal decomposition of the material. According to the mass spectrometer (HidenAnalytical HAL 201) mainly H_2 was released during this event. However the decomposition was not completed even if the temperature rose to 350 °C, therefore the material was heated again, this time up to 400 °C. The decomposition products were detected with the mass spectrometer, revealing formation of H_2, NH_3 and N_2. The interaction of amide/hydride anions is therefore possible at high temperature, however the

inspection of the sample revealed the formation of a shiny metal, suggesting that the powdered sample decomposed completely to form metallic potassium.

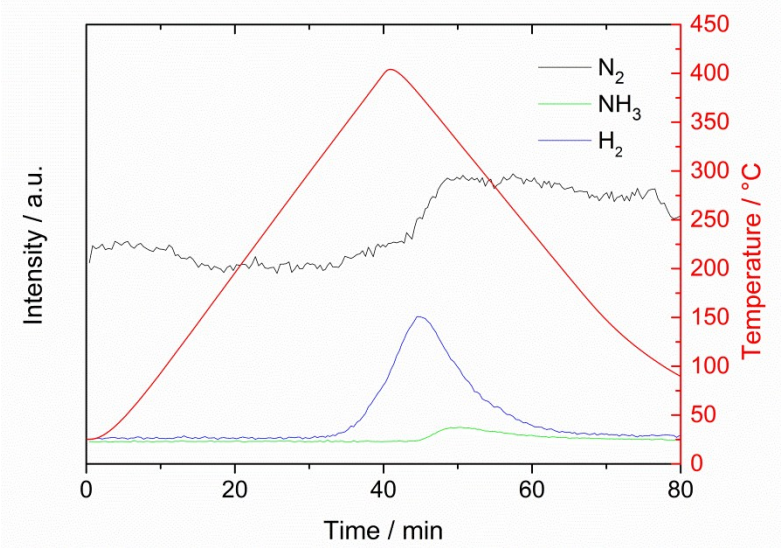

Figure S14. Mass spectrometer signal recorded on the gas flow during the thermal decomposition of the sample x = 0.5.

KNH_2[5] and KH[6] are reported to decompose above 320 °C and above 400°C respectively. However the present results show that, when combined, the two materials start to decompose already at 285 °C, indicating a possible interaction of the two anions to form H_2, while the nitrogen is released from the crystal structure in form of N_2 and NH_3.

References:

1. A. P. Hammersley, S. O. Svensson, M. Hanfland, A. N. Fitch and D. Hausermann, *High Pressure Res*, 1996, **14**, 235-248.
2. L. Lutterotti, S. Matthies, H. R. Wenk, A. S. Schultz and J. W. Richardson, *J Appl Phys*, 1997, **81**, 594-600.
3. V. Favre-Nicolin and R. Cerny, *Journal of Applied Crystallography*, 2002, **35**, 734-743.
4. A. C. L. a. R. B. V. Dreele, *Los Alamos National Laboratory Report LAUR 86-748*, 2000.
5. J. H. Wang, G. T. Wu, Y. S. Chua, J. P. Guo, Z. T. Xiong, Y. Zhang, M. X. Gao, H. G. Pan and P. Chen, *ChemSusChem*, 2011, **4**, 1622-1628.
6. M. Sale, C. Pistidda, A. Taras, E. Napolitano, C. Milanese, F. Karimi, M. Dornheim, S. Garroni, S. Enzo and G. Mulas, *Journal of Alloys and Compounds*, 2013, **580**, S278-S281.